Structures 80 (2025) 109833

Contents lists available at ScienceDirect

Structures

journal homepage: www.elsevier.com/locate/structures

Design and construction of concrete shells using semi-flexible auxetic grids as formwork

Amila Jayasinghe [a,b,*], Mohammad Hajsadeghi [c], Liyao Wan [c], John Orr [a], Raffaele Vinai [c], Prakash Kripakaran [c], Ken Evans [c]

[a] Department of Engineering, University of Cambridge, Cambridge CB3 0FA, UK
[b] School of Physics, Engineering and Computer Science, University of Hertfordshire, Hatfield AL10 9AB, UK
[c] Department of Engineering, University of Exeter, Exeter EX4 4QF, UK

ARTICLE INFO

Keywords:
Concrete shells
Structural optimisation
Auxetic
Novel construction methods
Shape optimisation

ABSTRACT

Concrete shells can be efficiently designed through form-finding techniques to create shapes where the structure functions predominantly in compression under the applied load. While such concrete shell floor systems can reduce material consumption by replacing traditional flexural load transfer with efficient membrane action, their construction is challenging with conventional formwork methods. This study conceptualises, develops, and experiments the use of flat auxetic grids as formwork for casting compressive-dominant concrete shells. Due to their negative Poisson's ratio, auxetic meshes exhibit dome-like synclastic behaviour, curving towards the same side in all directions when subjected to out-of-plane deformations. Therefore, the feasibility of transforming a flat auxetic grid into the most efficient shapes for concrete shells solely under the self-weight of concrete or with additional constraints is explored in this study. A parametric nonlinear finite element model linked to an evolutionary optimisation algorithm is developed to design a flat auxetic grid that deforms to approximate a form-found compression-dominant shell geometry. The construction of concrete shells using the designed auxetic geometry is experimentally demonstrated. A form-finding algorithm coupled with an evolutionary algorithm is also used to verify that the experimental geometries and the deformed finite element models of different auxetic formwork designs approach compression-dominant shell geometries. Results show that semi-flexible flat auxetic grids can be feasible, versatile, reusable, and less bulky as a formwork system for casting concrete into cast compression-dominant shell geometries.

1. Introduction

The construction industry is responsible for a significant share of carbon emissions from human activities, with cement production alone accounting for about 6 % of global carbon emissions [1]. Concrete is widely used in the construction industry, with an estimated annual consumption of 30 billion tonnes [2]. Several previous studies have shown that up to 75 % of carbon emissions from building construction are attributable to floors [3,4]. Concrete floor systems that transfer loads through flexure underutilise the concrete volume beneath the neutral axis, making them inefficient in terms of material consumption. In contrast, concrete shell floor systems can reduce material consumption by transferring loads through compression membrane action, efficiently utilising the properties of concrete, which performs well in compression but has weak tensile properties. Hawkins et al. [5] developed a shell floor system with textile-reinforced concrete groin vaults and pre-stressed steel ties, reducing self-weight by up to 53 % and embodied carbon by up to 58 % when compared to a conventional flat slab solution with similar capacity. Similarly, Rippmann et al. [6] demonstrated a material reduction of up to 70 % by adopting a funicular shell floor system. Adopting shell floor systems in concrete building design is a promising strategy for minimising material consumption and thus reducing carbon emissions. However, the inherent curved geometries in concrete shells pose challenges to construct with conventional rigid flat formwork methods. Therefore, this study explores a novel approach to constructing concrete shells using semi-flexible flat auxetic grids.

The optimum shell geometries to support uniformly distributed loads can be designed by form-finding, where shapes can be determined to purely transfer loads as a compression-dominant membrane without bending moments in the system [7,8]. Several form-finding methods

* Corresponding author at: School of Physics, Engineering and Computer Science, University of Hertfordshire, Hatfield AL10 9AB, UK.
E-mail address: jaas2@cam.ac.uk (A. Jayasinghe).

https://doi.org/10.1016/j.istruc.2025.109833
Received 13 May 2025; Received in revised form 18 July 2025; Accepted 28 July 2025
Available online 5 August 2025

have been developed and utilised to design concrete shells optimally, such as the Force Density Method, Thrust Network Analysis, and Dynamic Relaxation [9]. In this study, form-finding is performed by applying a uniformly distributed load over the entire surface, resulting in compression-dominant shell geometries when subjected to uniformly distributed loads.

For a given set of design criteria, there can be multiple different compression-dominant shell geometries. This versatility is reflected in the process of form finding; For a given floor panel shape, there can be several form-found compression-dominant shell geometries [9,10]. For example, Fig. 1 illustrates various form-found shapes for a shell covering a square base, where the shapes are designed using the Kangaroo [11] form-finding tool for the Rhino-Grasshopper [12] graphical programming interface. To generate each geometry in Fig. 1, a grid net with 30 divisions in both X and Y directions was used, and each node connecting to the closest nodes in horizontal, vertical, and diagonal directions with springs at 0^0, 90^0, and $\pm 45^0$. The four corners of the net were pinned (i.e. restrained translation in XYZ directions) and a uniformly distributed pressure was applied in Z direction. The Kangaroo plugin uses Dynamic Relaxation, and the different compression-dominant geometries in Fig. 1 are generated by varying the input parameters to the algorithm: support conditions on edges, properties of springs, and the applied load.

Despite the potential material savings, the curved geometries of shape-optimised concrete shell designs can be challenging to construct using traditional flat and rigid formwork methods. Despite researchers have been using various methods to manufacture concrete shells, these techniques need more investment for wider industry adoption [13]. Hawkins et al. [14] used custom-made timber formwork to cast textile-reinforced concrete shells. While rigid timber formworks for curved shell geometries can be bulky, their shell floor system was designed as groin vaults with four segments connected, each having a single curvature. Liew et al. [15] constructed a layout-optimised funicular concrete shell using a tailor-made formwork system using CNC milling and wire-cutting techniques for Expanded Polystyrene foam and timber. Meibodi et al. [16] fabricated a shell floor system with hierarchical ribs by concrete spraying a formwork which was assembled with 3D printed and CNC machined parts. While the aforementioned studies successfully fabricated shells to reduce concrete consumption in floor designs, the custom-made formwork was limited to the specific geometry for which it was designed and was often used only once.

Novel construction techniques have been explored by several researchers to fabricate shape-optimised concrete shells. Nuh et al. [17] fabricated a segmented doubly curved concrete shell where the geometry of each shell segment was formed using a moving-pin table and cast by spraying with a fibre-reinforced fine-grained concrete slurry. Kromoser et al. [18] reviewed different variations of pneumatic (inflatable) formwork to cast concrete shells and conducted large-scale experiments to illustrate the use of an active bending lifting pneumatic formwork. Rippmann et al. [6] designed and constructed a rib-stiffened segmented shell floor by 3D sand-printing the layout optimised geometry. Popescu et al. [19] also described a prototype concrete shell fabricated by concrete spraying a cable net and knitted formwork. The construction methods adopted in the studies above vary in terms of the need for special equipment, the bulkiness of the formwork, and the degree of customization required.

Auxetic materials have a negative Poisson's ratio, which means they contract and expand the transverse direction when subjected to axial compression and tension, respectively [20,21]. This counter-intuitive behaviour also results in synclastic shapes when auxetic grids are subjected to out-of-plane deformations, where the deformed geometries are curved toward the same side in all directions [22]. To achieve auxetic behaviour, conventional materials can be designed with geometric arrangements of their basic 'auxetic unit cells' in such a way that the relative movement of these units causes the overall material to expand laterally when stretched and contract laterally when compressed [23]. While there are several auxetic geometric arrangements commonly seen across literature, re-entrant honeycomb shapes are widely seen in studies concerning structural engineering applications [24–26]. Fig. 2 illustrates the difference between conventional and auxetic re-entrant honeycomb meshes when axial loads and out-of-plane loads are applied. To demonstrate the generic behaviour, linear Finite Element Models in Fig. 2 were analysed assuming the four corners are pinned (i.e., translations in XYZ are restricted, but rotations are unrestricted) and midpoint of the grid is displaced in Z direction by 1/8th of the span. Non-auxetic grids transform into saddle-shaped anticlastic geometries, while auxetic grids form dome-shaped synclastic geometries when subjected to out-of-plane forces. The exact deformed geometry and the curvatures in different directions of auxetic grid structures depend on the re-entrant geometric arrangement, as well as on the stiffness of the grid elements [27].

The versatility of the form-found concrete shell geometries (Fig. 1) and synclastic shapes possible from auxetic geometries (Fig. 2) suggest the possibility of using auxetic grids to design semi-flexible formwork for shape-optimised concrete shells. A recent study by Yan et al. [28] also explored the out-of-plane deformability of small-scale 3D printed auxetic meta-materials and hypothesised them as formwork for concrete shell geometries due to their characteristic synclastic behaviour.

This paper develops a novel formwork system for shape-optimised concrete shells using semi-flexible flat auxetic grids to approximate compression-dominant shell geometries when wet concrete is poured

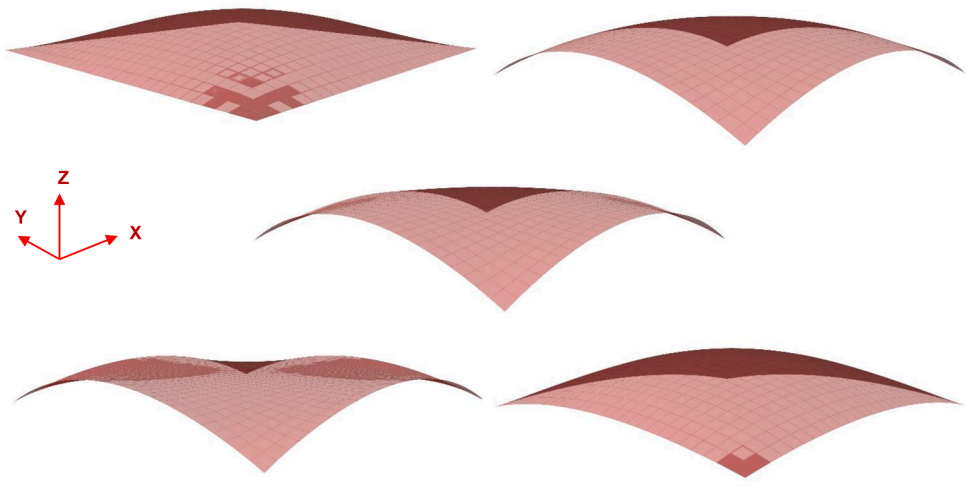

Fig. 1. Compression-dominant shell geometries to cover a square floor area: Form-found with Kangaroo [11] Form Finding Plugin for Rhino-Grasshopper [12].

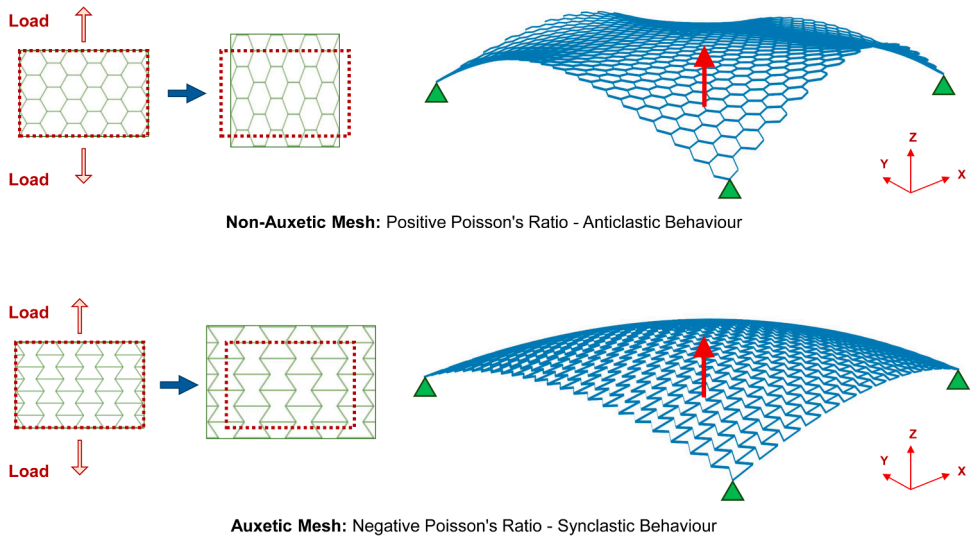

Fig. 2. The geometry of auxetic vs. non-auxetic meshes under out-of-plane deformation.

onto the formwork. In this context, semi-flexible refers to a formwork system that allows controlled deformation into desired shapes, without being fully rigid or overly flexible like a fabric. A design method for an auxetic grid geometry suitable for a formwork is devised, the construction process is illustrated for a shell floor panel with a span of 1.2 m, and the numerical models developed herein are experimentally validated. The span of 1.2 m for the prototype is selected based on the available laboratory space and the cost of the fabrication of the auxetic grid. Despite the deformations of the formwork auxetic grid, the planned concreted shell floor area was kept constant at 1.2 m × 1.2 m using falsework during the construction process.

2. Concept

This study utilises the synclastic nature of auxetic grids to approximate compression-dominant geometries in the design of a formwork system for concrete shells. The concept is that the auxetic cell geometry of the grid can be designed in such a way that the synclastic shape, achievable by applying the self-weight of wet concrete and/or minimal constraints, would result in structurally optimum shell shapes. To that end, a flat auxetic grid is developed herein to cast a concrete shell covering a square-shaped floor panel. The grid is pinned at its four corners (i.e., translation restrained in the XYZ directions, but rotations are unrestricted). The flat grid is designed to deform and approach the desired shell geometry when (a) a layer of wet concrete, up to the required shell thickness, is placed on the formwork and (b) midpoint of the grid is displaced in the Z-direction up to the required shell height, if necessary.

The use of an auxetic grid as a formwork for concrete shells requires solving two challenges (Fig. 3):

a) Modelling the synclastic behaviour of auxetic grid geometries when subjected to out-of-plane deformation.
b) Finding the concrete shell geometries with compression-dominant behaviour.

While auxetic grids exhibit synclastic behaviour, the exact overall geometry resulting from out-of-plane deformation depends on the auxetic cell geometry and the material properties of the grid, which can be estimated using non-linear finite element models. In another regard,

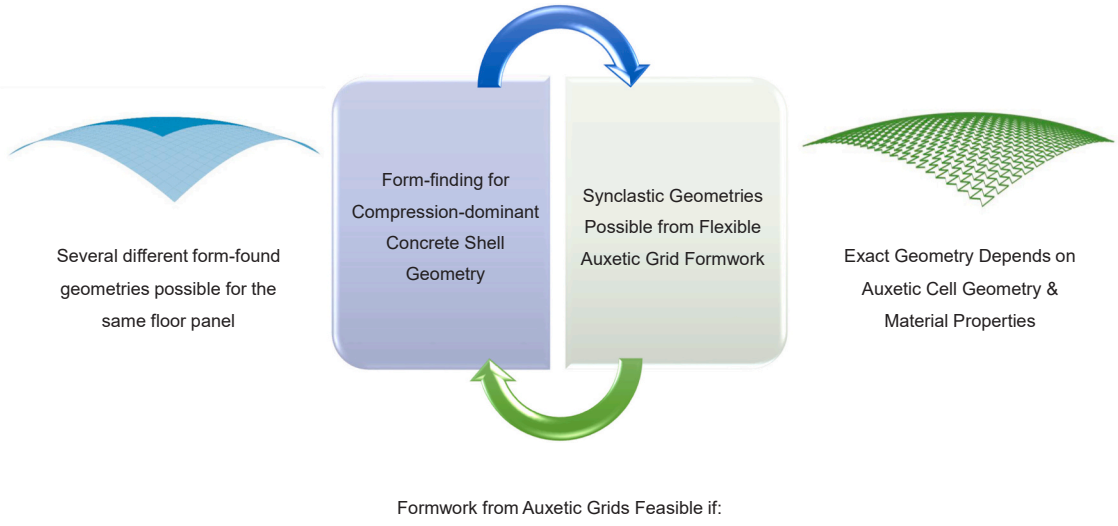

Fig. 3. Conceptualisation of auxetic grids as formwork for concrete shells.

several different compression-dominant shell geometries can be designed for the given floor area and the rise, using a form-finding algorithm with dynamic relaxation. Therefore, combining a parameterised form-finding algorithm and a parameterised finite element model could result in a potential auxetic grid geometry that can be deformed into a compression-dominant shell geometry with simple restraints. Once a feasible auxetic grid geometry is designed and fabricated, it can be used as a formwork by supporting at the corners and using a fabric to prevent concrete from seeping through the auxetic cells. This study explores the possibility of designing and constructing a flat auxetic grid to be used as a formwork for concrete shells where the grid can be deformed by the self-weight of wet concrete and minimal additional constraints to approximate a compression-dominant shell geometry.

Although there are many variables governing the deformed shape of the auxetic grid and the geometry of the compression-dominant shell determined by form-finding methods, the objective of matching the two shapes in this study is to leverage this large design space and versatility to develop a flat, semi-flexible formwork system for shells that can easily achieve structurally optimal shell shapes. Thus, for a given floor plan, it is important to note that there can be multiple different auxetic grids that may approximate compression-dominant shell geometries, which can differ from one another.

3. Design of formwork

The auxetic formwork grid in this study is designed using an interactive model which uses a heuristic optimisation algorithm, a form-finding algorithm, and a finite element model, as illustrated in Fig. 4. The model is created within the Rhino-Grasshopper [12,29]. A square-shaped panel with a span of 1.2 m is selected to illustrate the design and construction of concrete shells using an auxetic grid formwork where the grid is made of steel. The rise of the shell at the midpoint is set as 1/8th of the span, which is 150 mm. The auxetic grid geometry is selected as re-entrant honeycombs, and the cell size is kept the same across the whole area. The 2D re-entrant geometry is defined using the re-entrant angle and the number of cells in vertical and horizontal directions.

The Kangaroo [11] form-finding algorithm which uses the Dynamic Relaxation Method, is used to design a compression-dominant shell geometry to cover the area of 1.2 m × 1.2 m, as illustrated in Fig. 5. To match the nature of the synclastic shape auxetic grids transformed into (as in Fig. 2), the form-finding algorithm is used to find a compression-dominant membrane shape when the four edges are designed to be in the form of catenary curves. Fig. 5 also shows the spring arrangement, boundary conditions, and the variables used in the form-finding algorithm in this study. Thus, one form-found shape with a 150 mm rise at the midpoint is generated to be used as a reference optimal compression-dominant shell geometry in the process of designing the auxetic grid geometry in the next step.

Simultaneously, a parametric finite element model is developed for a re-entrant auxetic honeycomb grid to cover the same floor area of 1.2 m × 1.2 m using Karamba [30] FEA for Rhino-Grasshopper. The auxetic geometry is drawn based on the re-entrant angle and the number of cells in two perpendicular directions. The cell wall thickness and the grid height are selected as 2 mm and 6 mm respectively. This selection is informed by the accuracy of the available manufacturing methods and material availability for the experimental validations, further described in Section 3. The in-built material model in Karamba FEA [30] for Grade S275 mild steel is used here, with a modulus of elasticity of 210 GPa, a shear modulus of 80.8 GPa, and a tensile strength of 275 MPa. The version of Karamba FEA (Karamba3D 2.2.0.18) used in this study could not incorporate the non-linear behaviour of the material model but could consider geometric nonlinearity. As the non-linear behaviour is important in this context where a flat grid is deformed out-of-plane up to 1/8th of the span, the FEA model is programmed to account for geometric non-linear effects. The results are visualised to highlight the areas exceeding the utilisation of 100 % of the material strength, to identify the extent of potential plastic deformation for further investigation. Quadrilateral Shell elements were used to model the walls of the auxetic shells instead of beam elements to account for contribution of the shear deformation of the walls in the grid towards the overall deformation of the grid. The connections of grid walls at the nodes of the auxetic grid were modelled as fixed joints, restricting the relative translation and rotation in all directions.

As described in Fig. 6, the formwork system is idealised as an auxetic grid pinned at four corners (i.e., translation restricted in XYZ directions, but rotations allowed), allowing the grid to deflect under the weight of a 3 cm thick layer of concrete. The shell thickness of 3 cm is selected as a practical minimum shell thickness with the laboratory facilities, and to avoid accidental collapse. The load was applied as a uniformly distributed load in Z direction onto the grid, effectively applying vertical loads

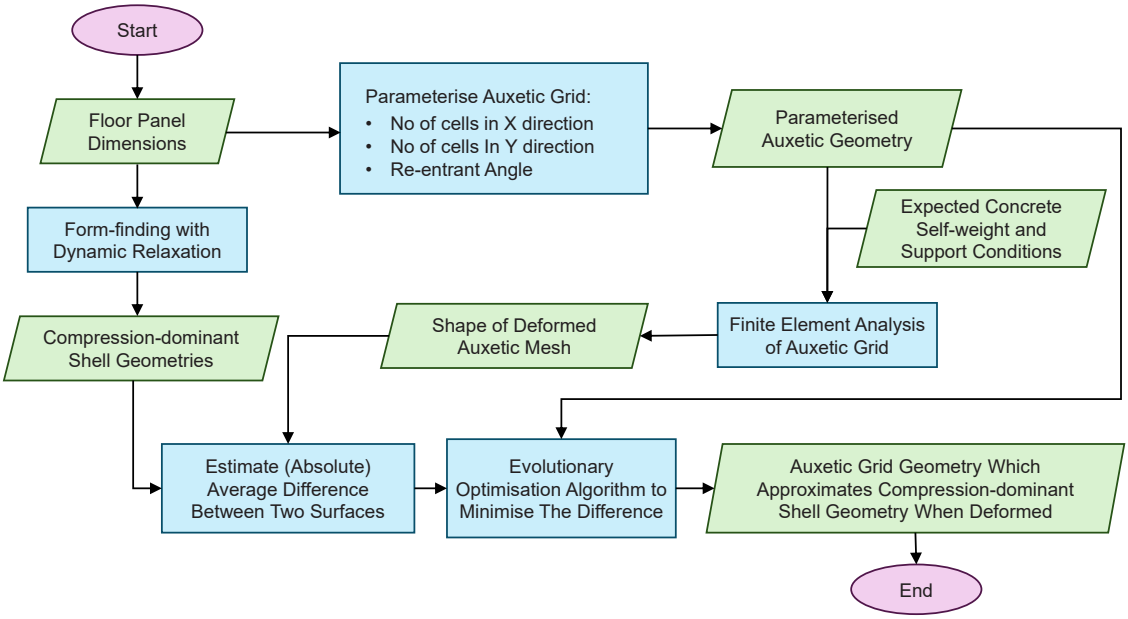

Fig. 4. Design approach for an auxetic grid as a formwork for compression-dominant concrete shell geometries.

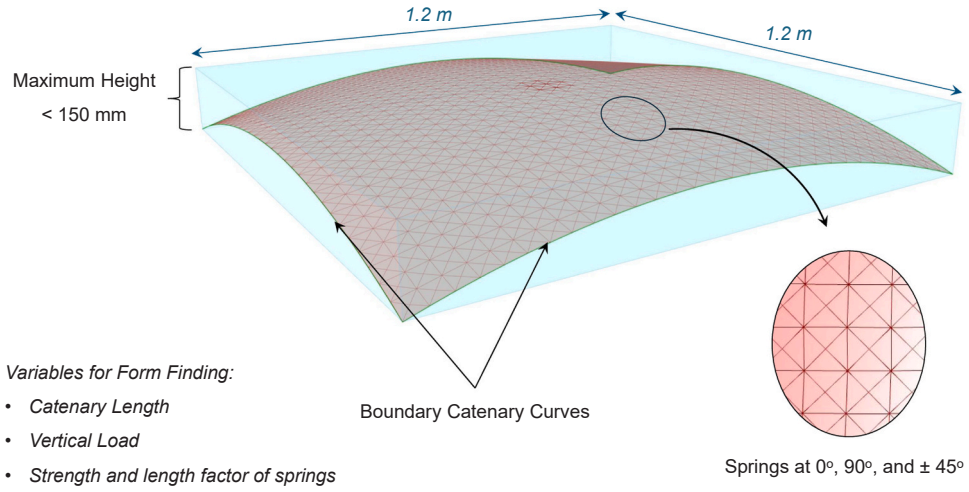

Fig. 5. Constraints for the form-finding algorithm.

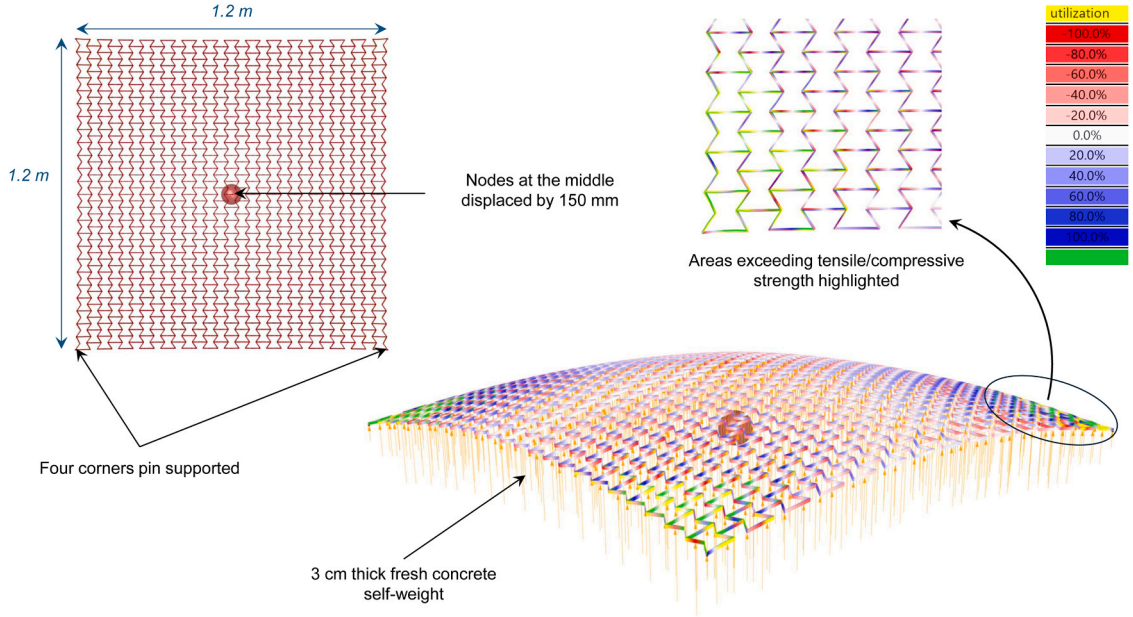

Fig. 6. Finite element model of the auxetic formwork grid.

at nodes in the finite element mesh across the auxetic grid. This applied load is transferred to the supports at corners by the auxetic grid through a combination of bending moments and axial forces across the grid, resulting in a deformation of the overall grid. Since the grid walls are expected to have bending and axial tensions due to the nature of loading rather than axial compression, the effect of buckling on the overall deformation is not considered at this stage of the study. Utilisation in the legend of Fig. 6 refers to the ratio between the strength of the material and the maximum equivalent stress in each face of the element. To ensure that the rise of the shell is 150 mm, a set of nodes at the midpoint is displaced by 150 mm as a support settlement. The legend is limited to ±100 % utilisation to highlight the areas of compression failure in yellow and tensile failure in green. Fig. 6 shows the deformed geometry upside-down to aid in conceptualising the system described here as a formwork for concrete shells.

To find the auxetic geometry for which the deformed shape approximately fits the reference form-found compression-dominant shell geometry, the Wallacei [31] optimisation tool in Rhino-Grasshopper is used. This plugin is an evolutionary algorithm based on the Non-dominated sorting genetic algorithm II (NSGA-II) [32]. The re-entrant angle and the number of cells in two perpendicular directions are input as genomes for optimisation, and the objective is set to minimise the difference between the reference form found surface and the deformed shape of the auxetic grid. The difference between the two shapes i.e. the objective function for the optimisation algorithm, is measured by calculating the average of the distances between (a) each node in the Finite Element Model of the auxetic steel grid, and (b) the closest point on the form-found surface to the point being considered. Since there are no other objective functions considered, a Pareto front is not considered in this study, and the solution with the minimum difference between the two surfaces is simply selected once the model is converged. Fig. 7 illustrates the converged solution where the reference form-found compression-dominant shell geometry is placed 100 % within the deformed geometry of the 6 mm thick auxetic steel grid. When calculating the average difference in this study, it is important to note that the best fit geometry, which refers to the surface with the minimum deviation, still results in a nonzero value. This occurs because the finite element model of the 6 mm thick grid includes nodes on both

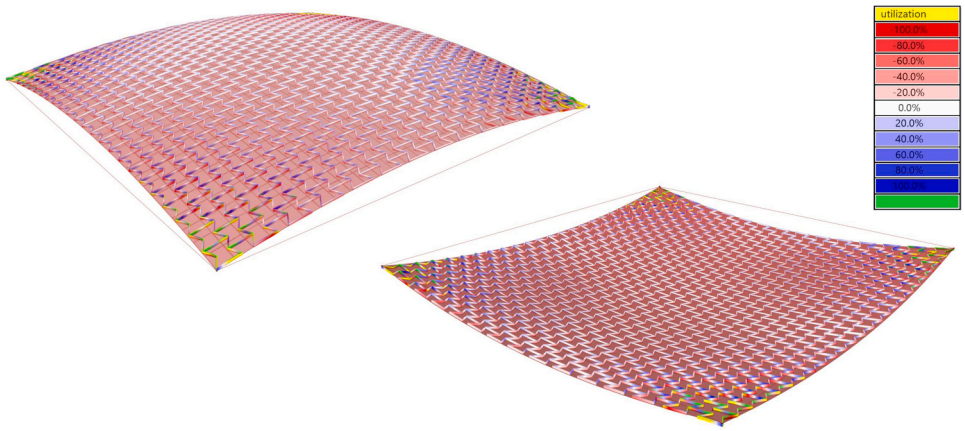

Fig. 7. Converged auxetic grid geometry with the minimal difference from the form-found shell geometry.

the top and bottom surfaces. The solution presented in Fig. 7 resulted in an average difference of 2.96 mm, which is approximately half the thickness of the grid, indicating a near perfect match. This converged geometry is used to design the experimental programme presented in Section 4.

4. Experimental illustration

The auxetic grid geometry designed in Section 3 is used to design the experimental prototype in this study, as shown in Fig. 8. The specimen is waterjet-cut from a flat 6 mm thick solid sheet of S275 Mild Steel, with a cell wall thickness of 2 mm. Solid circles with an 80 mm diameter are added at the four corners and the midpoint to incorporate the supports and deformations, respectively. Since the Finite Element Analysis in Figs. 6 and 7 indicates the possible yielding of some regions close to the supports, the wall thickness of some cells in that area is adjusted to increase the width and gradually merge into the average wall thickness, to prevent accidental collapse. While the variations adopted herein are heuristic to some degree, the objective is to develop a safe experimental prototype to proceed with the experiments, with the possibility of being used for multiple experiments without collapse. Further studies are needed to determine the effect of such variations, sensitivity on the overall behaviour, and the minimum required alterations of the shape.

This auxetic grid is used to perform three experimental tasks:

a) Apply pin supports at the four corners, displace the midpoint up to 150 mm, and measure deformation across the grid.
b) Use the auxetic grid to cast a concrete shell while supporting the midpoint at a 150 mm displacement (**Shell 1**).
c) Use the auxetic grid to cast a concrete shell after removing the support at the midpoint to allow deflection purely due to the self-weight of wet concrete (**Shell 2**).

The first task above is performed to validate the nonlinear finite element model by comparing it with the experimentally deformed shape of the auxetic grid. The pin supports have a 30 mm distance from the centre of rotation to the top surface of the support and allow for a 90° rotation in one direction. These supports are aligned so that their direction of rotation is pointed toward the centre of the grid, as shown in Fig. 9(a). The displacement at the midpoint is gradually increased from 0 mm (keeping the grid flat relative to the supports) to 150 mm using a screw system, and the deformations across the grid are monitored using 105 LEDs connected to a dynamic measuring system.

The second and the third experimental tasks, casting Shell 1 and Shell 2, are to illustrate the use of a flat auxetic steel grid as a formwork for concrete shells and to assess the feasibility of achieving compression-dominant shell geometries. Once cured, the two concrete shells are 3D scanned to compare with the finite element model and then the best-fit compression-dominant shell geometry. Fig. 9 shows the steps of the

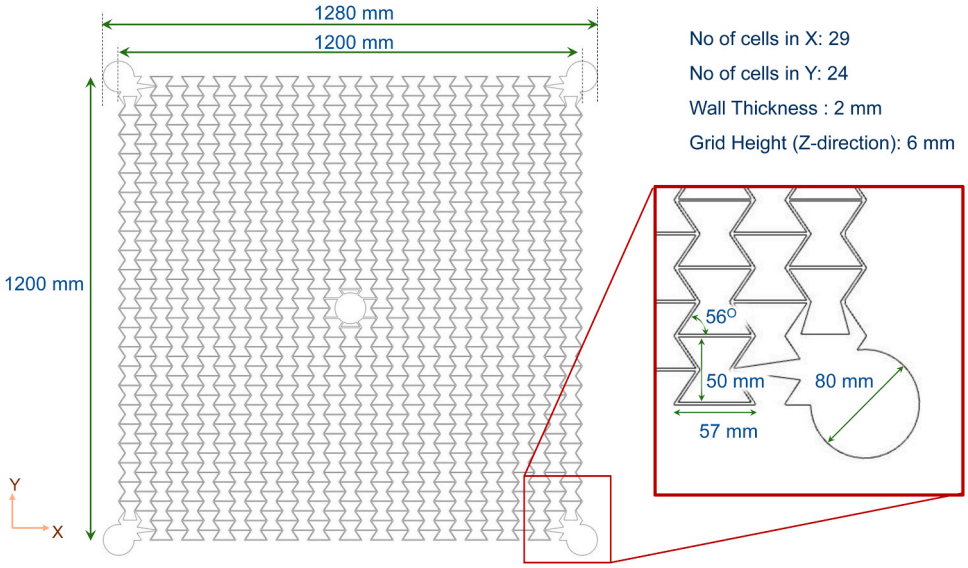

Fig. 8. Schematic of the auxetic grid used in the experimental programme.

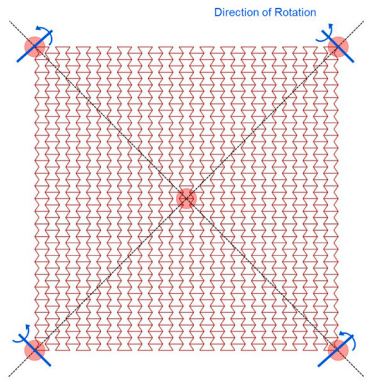

Step 1 - Pin support the auxetic grid from four corners

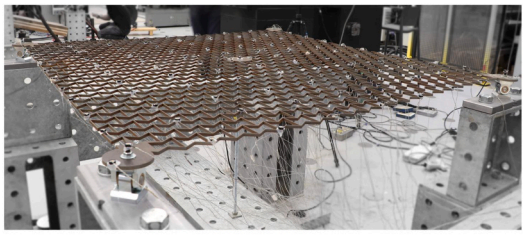

Step 2 - Measure deflection across the grid with LEDs when the midpoint is displaced from 0 mm until 150 mm

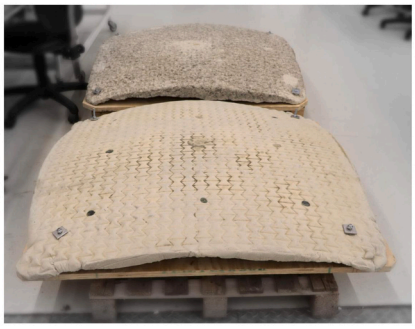

Shell 1: (Middle Supported at 150 mm)

Shell 2: (Middle not supported- deformed due to self weight)

Step 3 - Cast concrete shells using auxetic grid as a formwork

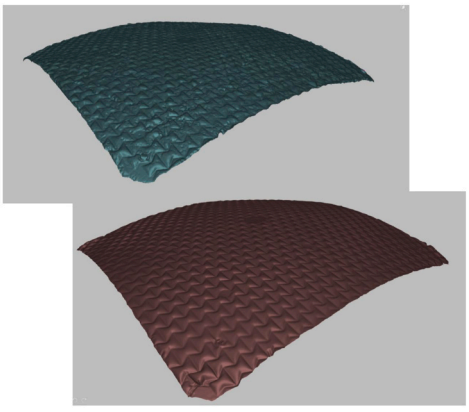

Step 4 - 3D Scan the geometry of the concrete shells

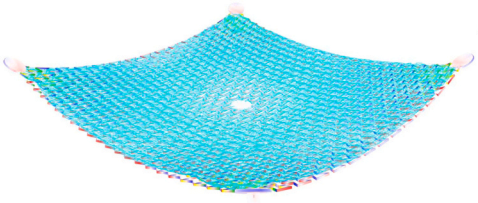

Step 5 - Compare the 3D scanned experimental geometry with FEA of auxetic formwork

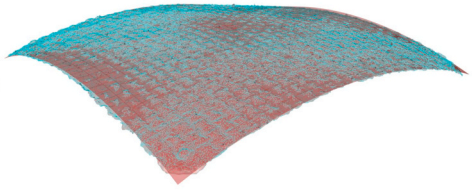

Step 6 - Compare the 3D scans with best-fit form-found compression-dominant shell geometry

Fig. 9. Methodology to assess the feasibility of auxetic grids as formwork for concrete shells.

experimental and computational methodology adopted.

The procedure of casting Shell 1 is also described in Fig. 10, where Expanded Polystyrene sideboards and Polyester fabric are used to transform the auxetic grid into a formwork. After the previous experimental stage, during which the midpoint of the grid was vertically displaced by 150 mm, the screw system at the midpoint remained unchanged to maintain the concrete shell height at 150 mm. A polyester fabric was laid over the auxetic grid to prevent concrete from seeping through. To ensure a consistent concrete shell thickness of 30 mm, 3D-printed plastic cover blocks were attached to the fabric at multiple points. The concreting of the shell was then carried out manually. When casting Shell 2, a similar procedure is adopted without supporting the midpoint of the grid. Fine-grained concrete mixes (without coarse aggregates) are used for both shells, whereas the mix for Shell 1 is reinforced with 1 % by volume of 25 mm long GFRP fibres. Both concrete mixes were designed to have sufficient workability to allow for manual casting of the shells. The objective was to test different concrete mixes with the proposed formwork method. Hypothetically, the properties of the concrete mix, apart from its density, should not affect the performance of the formwork system. The experimental concrete compressive strength and density for Shell 1 are 18 MPa and 1940 kg/m^3, whereas those for Shell 2 are 48 MPa and 2100 kg/m^3. The low concrete densities are due to the absence of coarse aggregates in both mixes and the porous matrix induced by fibres for the mix in Shell 1. The resulting concrete shells have synclastic geometries and architectural features imprinted from the auxetic grid formwork, as presented in Fig. 11.

5. Results and analysis

The finite element model is adjusted to incorporate the measured deviations between the physical model and the initial design described in Section 3, as shown in Fig. 12. The solid circles at the corners are added to the finite element model. Due to the 30 mm height of the pin support between the centre of rotation and the connecting surface of the grid, horizontal translations occur at the four corners of the grid, resulting in changes compared to the initial model. Therefore, the pin

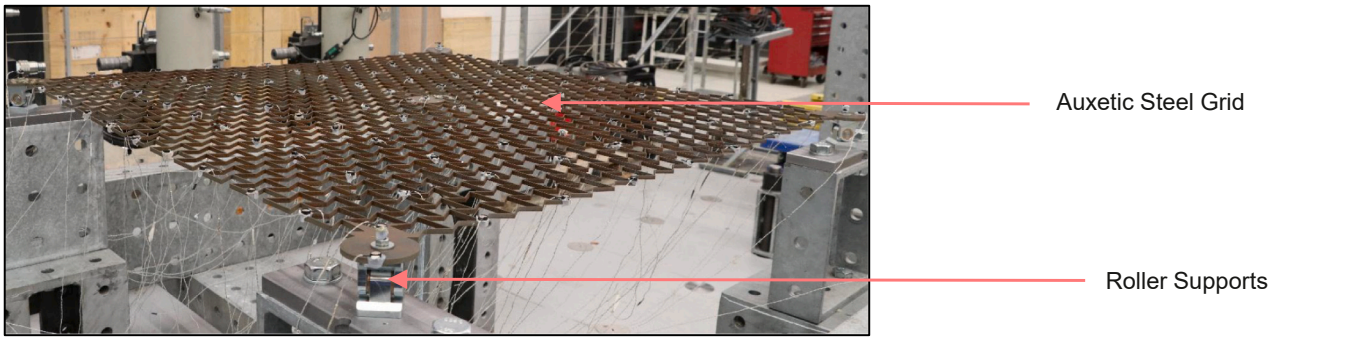

(a) Auxetic Steel Grid Supported from four corners and propped at the middle

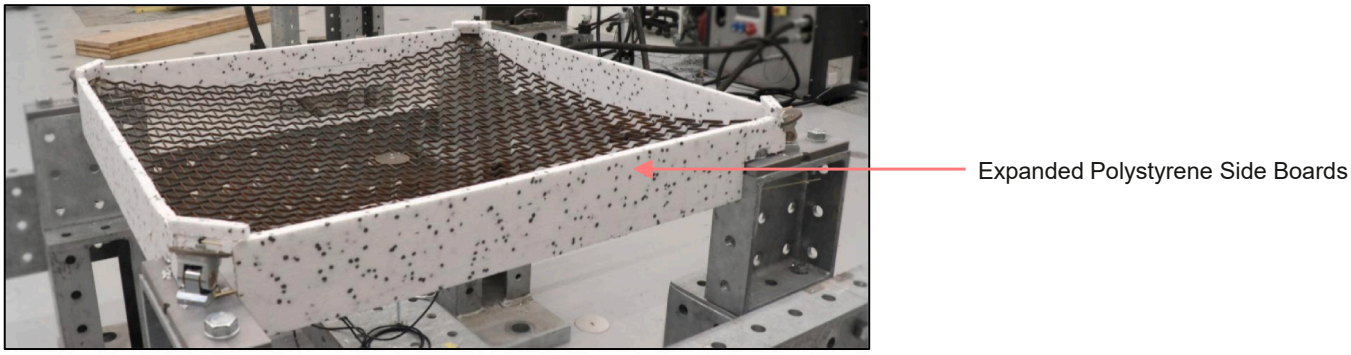

(b) With midpoint moved by 150 mm and sides supported with EPS boards

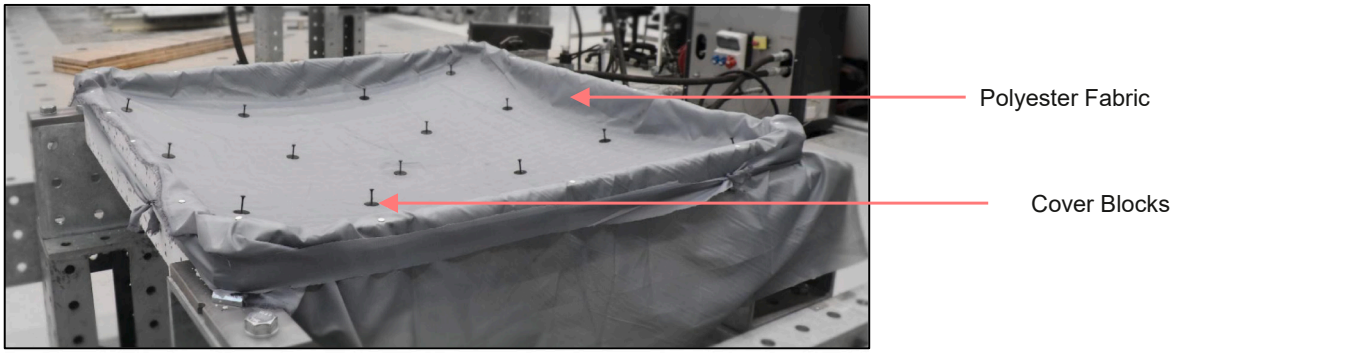

(c) Fabric and cover blocks to complete the formwork

(d) Concreting the shell

Fig. 10. Procedure of casting Shell 1.

Fig. 11. Concrete shell (Shell 2) cast using an auxetic grid as a formwork.

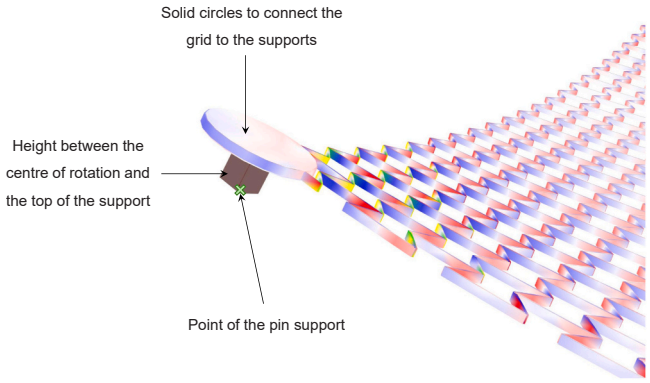

Fig. 12. Adjusted finite element model of the pin support at the corners of the auxetic grid for validation of experiments.

supports are modelled as 30 mm tall bars fixed (no translation and rotation are allowed) to the solid circles at the four corners while pinning (translations in XYZ is restricted while rotations are unrestricted) the bottom end of the bars.

The difference between the experimental displacement readings from the LEDs across the grid and the deformation according to the finite element model is shown in Fig. 13. While the displacements are monitored throughout while the displacement at the midpoint is increased from 0 mm to 150 mm, this figure shows two instances where the displacement at the midpoint is 100 mm and 150 mm. Out of 105 nodes monitored, only 4 nodes show more than a 10 mm difference when the midpoint is at 100 mm, and only 7 nodes exceeded a 10 mm difference when the midpoint is at 150 mm, indicating a reasonable accuracy of the finite element model. Fig. 14 illustrates the difference between the 3D scanned models of both the concrete shells and the respective deformed shapes of the finite element models. For this comparison, the self-weight of concrete for each shell is adjusted in the finite element model based

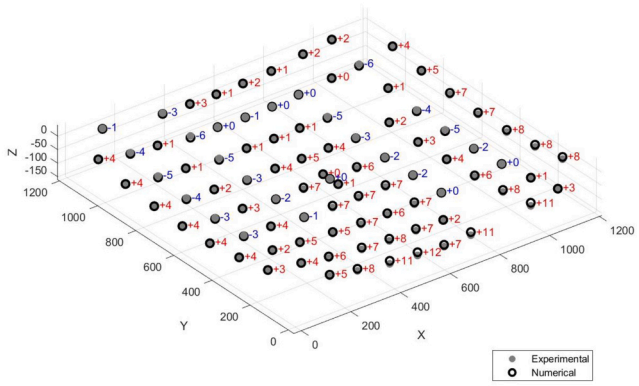

(a) When displacement at the Centre is 100 mm

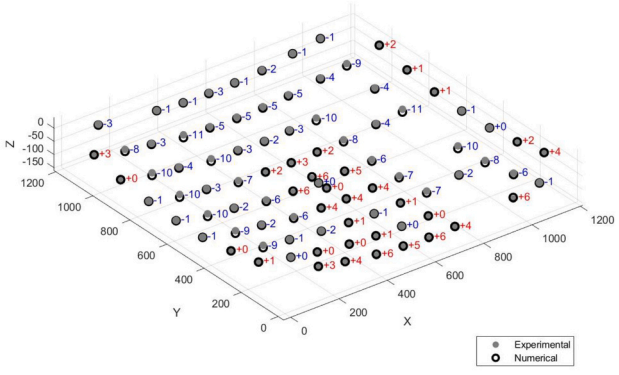

(b) When displacement at the Centre is 150 mm

Fig. 13. Difference in vertical displacement between the experiment and FEA.

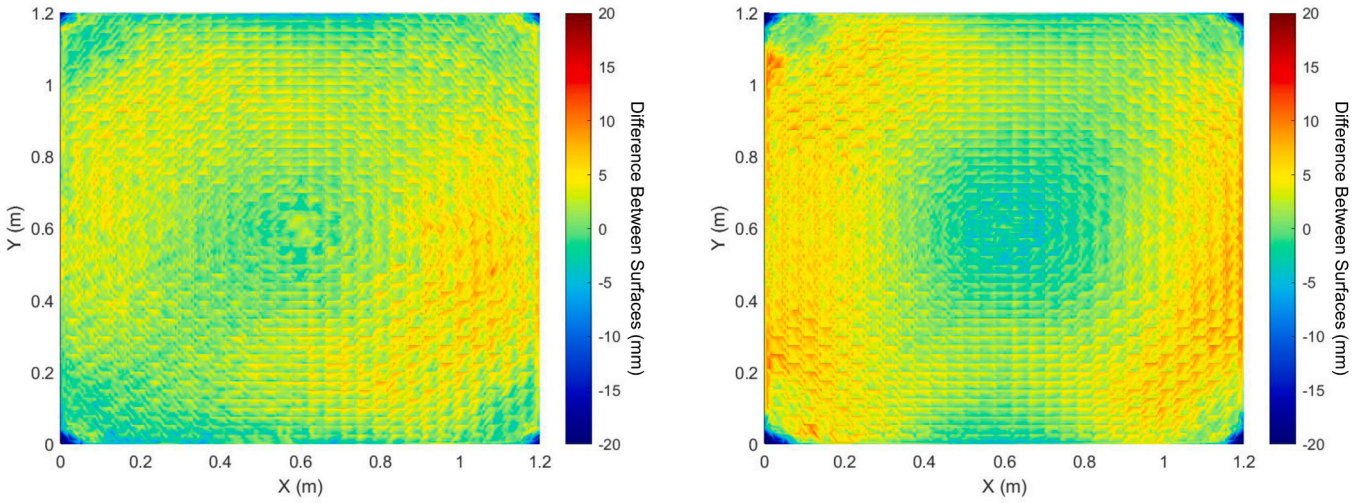

Fig. 14. Difference between the 3D-scanned experimental geometry of concrete shells and FEA of the auxetic grid.

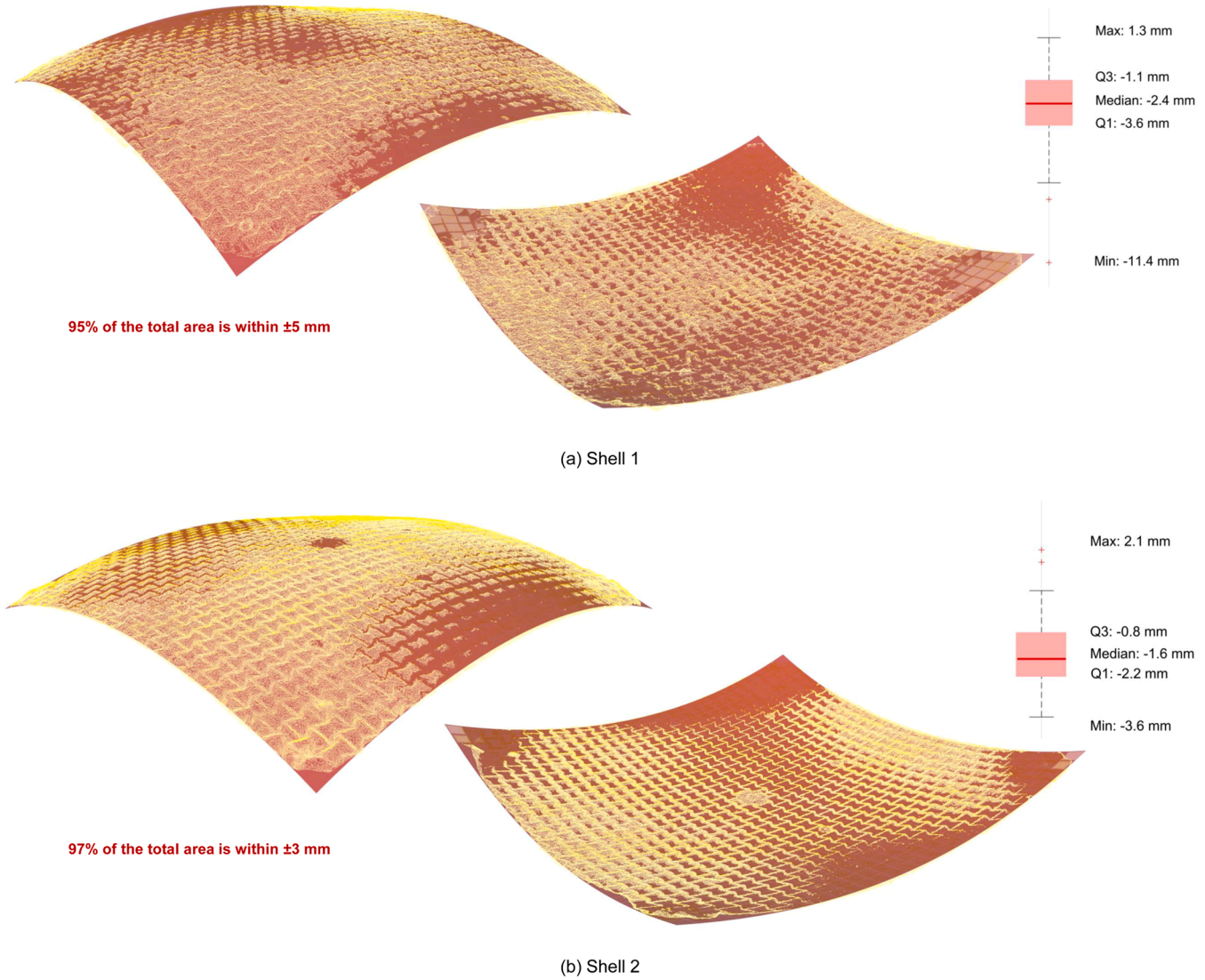

Fig. 15. Difference between the 3D-scanned experimental geometry of concrete shells and the best-fit form-found compression-dominant shell geometry.

on the experimental weight of the total shell. The height to the midpoint of Shell 1 is 150 mm as the midpoint is fixed at this level, whereas the height of Shell 2 is 180 mm when the formwork deflected purely due to the self-weight of wet concrete. The finite element models closely matched the experimental geometries, with Shell 1 showing 94 % of the area within a $\pm$ 7 mm difference, while Shell 2 showed 88 % of the area within the same range. It is also worth noting that the steel auxetic grid showed negligible permanent deformation after all the stages of the experimental programme, highlighting the potential of reusing the grid as a formwork.

Although the initial design method for the auxetic grid as formwork was developed using a single form-found optimum concrete shell geometry, the same grid was used to cast two different concrete shells with varying support conditions. While the initial assumption considered all four corners to be pinned, it was observed that horizontal translations induced by the height of the hinges in the experimental setup also influenced both the final shape and the bending stiffness of the grid. Nevertheless, the core objective of this study is to leverage the synclastic behaviour and the resulting versatility of auxetic grids to cast compression-dominant concrete shells. Accordingly, the experimental shell geometries obtained in this study were compared with best-fit form-found shell geometries. The supports were not used as reference points for the comparison in this analysis because the shell concreting did not extend fully to the corners. Certain areas at the grid's corner points were intentionally left unconcreted to maintain access to the connections required for demoulding. Instead, the 3D scanned surface was compared using the midpoint of the shell as the reference point.

The geometries of both shells are 3D scanned using an Artec3D Leo handheld scanner and compared with best-fit compression-dominant shell geometries, in Fig. 15. Since the shape of Shell 1 is governed by the

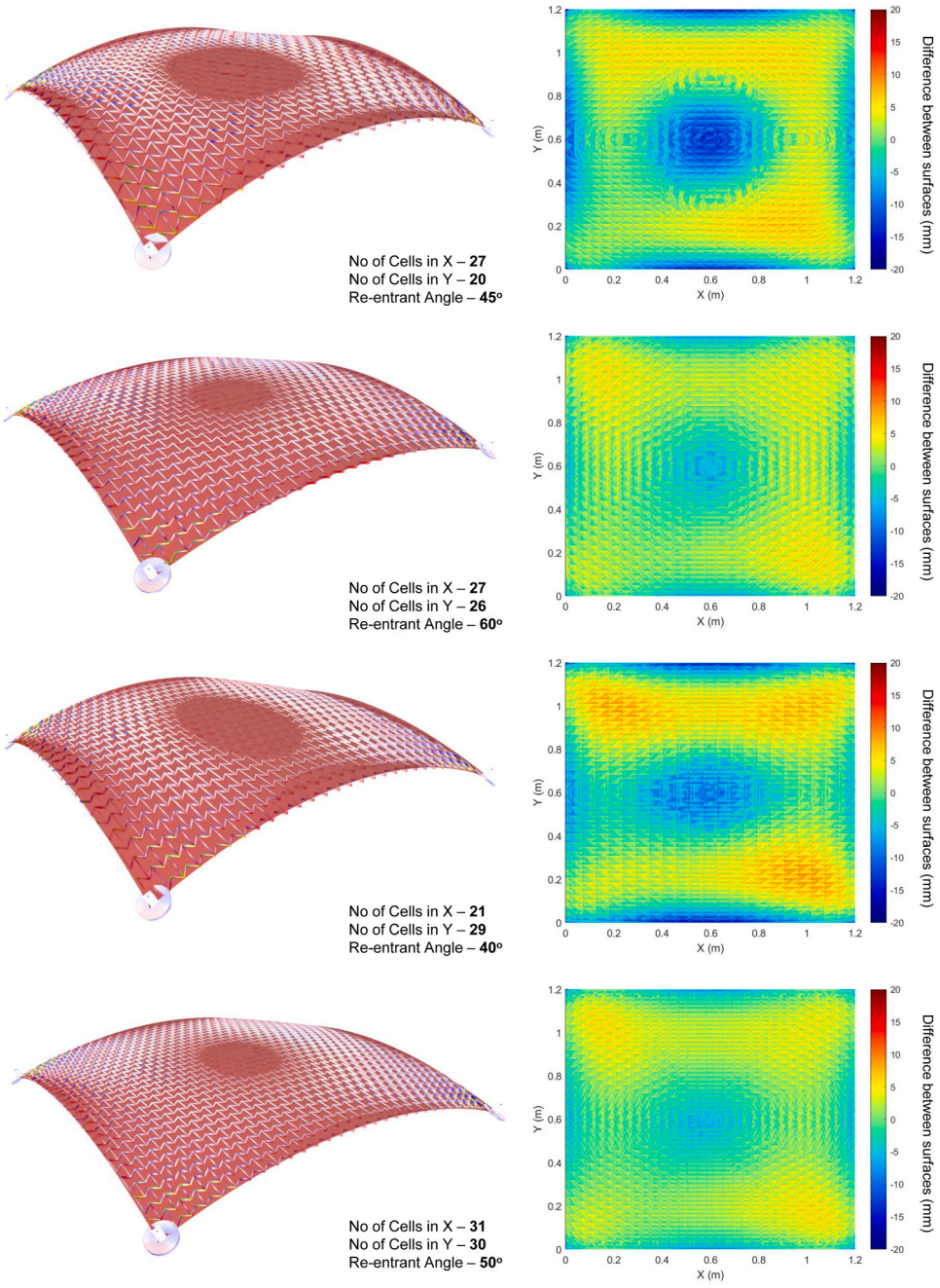

Fig. 16. Difference between the FEA of different auxetic grid geometries and their respective best-fit form-found compression-dominant shell geometries.

weight of the wet concrete and the support at the midpoint whereas Shell 2 is shaped mainly by the self-weight, this comparison is carried out to understand whether different formwork arrangements with the same auxetic grid could result in satisfactory compression dominant shell geometries. The Kangaroo form-finding tool is used to generate compression-dominant surfaces while Wallacei [31] evolutionary optimisation algorithm is used to optimise the result from Kangaroo to minimise the difference with the 3D scanned experimental shell geometry. The difference between the two surfaces is defined as the average distance from each point on the 3D scanned geometry to the closest point on the form-found surface. Some differences between the form-found surface and the 3D scanned surface are to be expected due to the auxetic cell features imprinted by the grid formwork due to the fabric draping in the auxetic cells, as in Fig. 10. Of the total area, 95 % of Shell 1 is within ± 5 mm of the best-fit form found surface, while 97 % of Shell 2 is within ± 3 mm of its best fit. The box-whisker plots in Fig. 15 are also presented to highlight the potential of achieving different compression-dominant shell geometries with the same flat auxetic steel grid formwork.

The features of the resulting synclastic shape are influenced by the geometrical properties of the auxetic mesh. For the same floor panel area of 1.2 m × 1.2 m, Fig. 16 shows the finite element analysis of different auxetic grid geometries once the midpoint is displaced and supported at 150 mm, and loaded with a 3 cm thick concrete layer. For each grid, the best-fit compression-dominant form-found surface is also identified and the difference between the two surfaces is presented. Since synclastic geometries can be asymmetric for some auxetic grids, the form-finding algorithm is modified to treat the lengths of the catenary curves in perpendicular directions as independent variables. The deformed shapes of the four grids considered (from top to bottom) show 93 %, 99 %, 95 %, and 99 % of total area within less than ±10 mm difference from the best-fit compression-dominant geometry. Although Fig. 15 clearly shows geometric discrepancies between the best-fit form-found geometry and the deformed shape of the auxetic grid in several areas, 93–99 % of the shell surface exhibits deviations of less than ±10 mm. For a concrete shell spanning 1.2 meters, constructing it with a thickness smaller than this deviation is practically unfeasible. Therefore, despite the observed differences, a concrete shell built using the auxetic grid as formwork will still accommodate a complete compressive membrane within its thickness. This shows that while some re-entrant auxetic geometries will result in synclastic geometries closer to compression-dominant shell geometries than other auxetic geometries, the differences may be still negligible. Considering that these deviations might be insignificant considering the minimum feasible thicknesses of concrete shells due to the construction tolerance and safety, auxetics grids present a promising method to cast concrete shells from a flat semi-flexible formwork.

This study experimentally and numerically illustrated the successful use of auxetic geometries to design a grid formwork to achieve compression-dominant shell geometries with minimal additional constraints. The developed formwork system presents opportunities to construct concrete shells with a flat semi-flexible grid without a rigid bulky formwork. The proposed formwork system showed high versatility in delivering compression-dominant shell shapes, which could be obtained with different loads and support conditions on the same mesh, as well as changing the geometrical parameters of the auxetic mesh itself. Since this paper focuses on concrete shell geometries optimised for uniformly distributed loads, further investigations are needed to explore the effect of eccentric loads on the design and feasibility of auxetic grid formwork.

Whilst this study demonstrated the suitability of flexible auxetic formwork to cast a square-shaped concrete shell with a 1.2 m span, further research is required to investigate the scalability of the auxetic grids as formwork and the applicability for different shell shapes. This paper used an auxetic steel grid with 2 mm thick and 6 mm tall cell walls which provided the required degree of flexibility to cast shells with 1.2 m span. The preliminary computational studies suggested that a similar steel grid scaled down to cast a shell with 0.5 m span may be too rigid as an auxetic formwork to achieve desirable shell geometries, but shells in such scale is rarely used in structural applications. Simply scaling up the proposed system for a shell floor system on a practical building would be infeasible due to both the manufacturing of the auxetic grid as a single unit and achieving the deformations towards desired shell shapes without collapse due to steel yielding. However, the proposed system can be hypothetically used to cast a large-scale floor system as a collection of different grid elements with a supporting falsework, similar to the concept discussed by Yan et al. [28]. Thus, further studies are necessary to develop an auxetic formwork system for a large-scale application.

Out-of-plane bending stiffness plays a crucial role in the feasibility of the proposed auxetic formwork method for concrete shells. While the material properties of the grid and the auxetic geometry directly govern the bending stiffness of the auxetic formwork as expected, it was observed that the experimental considerations at the supports played a significant role. The initial finite element modelling of the proposed formwork system (Fig. 6 & 7) assumed pinned support conditions (translations restricted but rotations allowed in XYZ directions) at the four corners. However, the experimental setup of pinned supports would inevitably have a height between the centre of rotation and the connecting point of the grid (Fig. 12). While the experimental setup adopted in this study used available hinges in the market, the impact on the stiffness by the translation induced due to the rotations of hinges could be observed. Unlike a grid that is ideally pinned at all four corners, the rotation of the hinges causes the corner points of the grid to move toward its centre, allowing it to deform under less load. In this study, a steel grid with a span of 1.2 m supported by roller supports with 30 mm height (between the rotating centre and the top of the support) had bending stiffness ideal for a formwork to allow the deformation only under the self-weight of the wet concrete. However, further studies are needed to understand the bending stiffness and its impact on the feasibility of the proposed formwork.

This paper presents a novel concept to construct shape-optimised concrete shells using flat semi-flexible auxetic grids as formwork and performed several experiments as proof of concept. Thus, the focus of this paper is to present the conceptualisation, develop a design methodology, and experimentally illustrate the feasibility of the novel approach developed herein. Therefore, while the numerical and computational plugins have been used in Rhino-grasshopper models designed in this study, the focus has largely been on the development of the experimental prototype and the experimental proof of concept. There are multiple areas of further research needed about the out-of-plane stiffness vs technical feasibility, scalability, accuracy of the heuristic optimisation models, geometric nonlinearity, plastic deformations of the auxetic grids, and the impact of the support conditions. While the authors are further investigating the above aspects, the developed computational models are available in the supplementary materials for the benefit of interested readers.

6. Conclusions

This paper described the results obtained by designing and testing a square-shaped auxetic mesh with a span of 1.2 m, whose synclastic deformation could approximate compression-dominant shell geometries. The predictions from a non-linear finite element analysis are validated by experimental illustrations through monitoring overall deformations when the midpoint of the grid is displaced and by 3D scanning shells cast using the grid as formwork. Two concrete shells are cast using the same flat auxetic steel grid: one by applying simple geometric constraints, and the other by allowing the mesh to deform solely under the self-weight of fresh concrete. Both resulting concrete shells deviate by no more than ±5 mm over up to 95 % of surface area when compared to the best-fit compression-dominant shell geometries designed for

uniformly distributed loads.

Semi-flexible flat re-entrant auxetic steel grids can be successfully used as formwork to cast concrete shells with compression-dominant geometries. The synclastic behaviour of auxetic grids can be harnessed to design a formwork system in which a flat grid transforms into a compression-dominant shell geometry, defined for uniformly distributed loads, using only the self-weight of wet concrete or minimal additional constraints such as displacing the midpoint. While a particular auxetic grid can be used to create multiple different feasible shell shapes by changing the applied constraints, different auxetic geometries for the same set of constraints can result in different compression-dominant shell shapes.

This paper shows that a parametric finite element model connected to an evolutionary optimisation algorithm can be used to design a flat auxetic grid, which can be easily deformed to approximate a form-found compression-dominant shell geometry. A form-finding algorithm connected to an evolutionary algorithm can be used to verify that the deformed geometry of different auxetic grids under different loading and supporting conditions approach compression-dominant shell geometries. Since the grid used in the experiments herein also does not exhibit significant plastic deformation after multiple uses, the proposed formwork system may offer a reusable and versatile method to cast concrete shells with optimum geometries. Therefore, the presented formwork system with a semi-flexible auxetic grid as a formwork is a feasible, versatile, reusable, and less bulky method to cast concrete shells with optimum compression-dominant shell geometries. Further research is needed to develop practical manufacturing methods for the auxetic meshes and to clarify the relationship between the grid stiffness and the loading conditions resulting in compression-dominant membranes.

CRediT authorship contribution statement

Liyao Wan: Writing – review & editing, Investigation, Conceptualization. **John Orr:** Writing – review & editing, Supervision, Resources, Project administration, Methodology, Investigation, Funding acquisition, Conceptualization. **Amila Jayasinghe:** Writing – original draft, Visualization, Validation, Software, Methodology, Investigation, Formal analysis, Data curation, Conceptualization. **Mohammad Hajsadeghi:** Writing – review & editing, Investigation, Conceptualization. **Raffaele Vinai:** Writing – review & editing, Supervision, Resources, Project administration, Methodology, Investigation, Funding acquisition, Formal analysis, Conceptualization. **Prakash Kripakaran:** Writing – review & editing, Supervision, Resources, Methodology, Investigation, Formal analysis, Conceptualization. **Ken Evans:** Writing – review & editing, Supervision, Resources, Project administration, Funding acquisition, Conceptualization.

Declaration of Competing Interest

The authors declare that they have no known competing financial interests or personal relationships that could have appeared to influence the work reported in this paper.

Acknowledgements

The work presented in this paper was part of the SHUTTERING research project funded by the Engineering and Physical Sciences Research Council (EPSRC) (EP/W019027/1). The authors would like to acknowledge and thank the contributions of the NRFIS laboratory team Dr. Pieter Desnerck, Ricardo Osuna-Perdomo, and other supporting staff.

Data availability

All data created during this research are openly available from the University of Cambridge data archive at https://doi.org/10.17863/CAM.120062.

References

[1] UNFCCC. Bigger Climate Action Emerging in Cement Industry | UNFCCC. UN Climate Change News 2017. ⟨https://unfccc.int/news/bigger-climate-action-emerging-in-cement-industry⟩ (accessed July 8, 2020).
[2] Monteiro PJM, Miller SA, Horvath A. Towards sustainable concrete. Nat Mater 2017;16:698–9. https://doi.org/10.1038/nmat4930.
[3] Sansom M, Pope RJ. A comparative embodied carbon assessment of commercial buildings. Struct Eng 2012;90:38–49.
[4] Foraboschi P, Mercanzin M, Trabucco D. Sustainable structural design of tall buildings based on embodied energy. Energy Build 2014;68:254–69. https://doi.org/10.1016/j.enbuild.2013.09.003.
[5] Hawkins W, Orr J, Ibell T, Shepherd P. A design methodology to reduce the embodied carbon of concrete buildings using thin-shell floors. Eng Struct 2020;207:110195. https://doi.org/10.1016/j.engstruct.2020.110195.
[6] Rippmann M, Liew A, Van Mele T, Block P. Design, fabrication and testing of discrete 3D sand-printed floor prototypes. Mater Today Commun 2018;15:254–9. https://doi.org/10.1016/j.mtcomm.2018.03.005.
[7] Tomás A, Martí P. Shape and size optimisation of concrete shells. Eng Struct 2010;32:1650–8. https://doi.org/10.1016/j.engstruct.2010.02.013.
[8] Bellés P, Ortega N, Rosales M, Andrés O. Shell form-finding: physical and numerical design tools. Eng Struct 2009;31:2656–66. https://doi.org/10.1016/j.engstruct.2009.06.013.
[9] Congiu E, Fenu L, Briseghella B. Comparison of form-finding methods to shape concrete shells for curved footbridges. Struct Eng Int 2021;31:527–35. https://doi.org/10.1080/10168664.2021.1878974.
[10] Adriaenssens, Sigrid, Block, Philippe, Veenendaal, Diederik, et al. Shell Structures for Architecture: Form Finding and Optimization. n.d.
[11] Piker D. Kangaroo: form finding with computational physics. Archit Des 2013;83:136–7. https://doi.org/10.1002/ad.1569.
[12] Robert McNeel & Associates. Grasshopper - algorithmic modeling for Rhino. 2021.
[13] Jayasinghe A, Orr J, Ibell T, Boshoff WP. Comparing the embodied carbon and cost of concrete floor solutions. J Clean Prod 2021;324:129268. https://doi.org/10.1016/j.jclepro.2021.129268.
[14] Hawkins W, Orr J, Shepherd P, Ibell T. Design, construction and testing of a low carbon Thin-Shell concrete flooring system. Structures 2019;18:60–71. https://doi.org/10.1016/j.istruc.2018.10.006.
[15] Liew A, López DL, Van Mele T, Block P. Design, fabrication and testing of a prototype, thin-vaulted, unreinforced concrete floor. Eng Struct 2017;137:323–35. https://doi.org/10.1016/j.engstruct.2017.01.075.
[16] Meibodi MA, Jipa A, Giesecke R, Shammas D, Bernhard M, Leschok M, et al. Smart slab: computational design and digital fabrication of a lightweight concrete slab. Recalibration on Imprecision and Infidelity - Proceedings of the 38th Annual Conference of the Association for Computer Aided Design in Architecture. Mexico City: ACADIA; 2018. p. 434–43.
[17] Nuh M, Oval R, Orr J, Shepherd P. Digital fabrication of ribbed concrete shells using automated robotic concrete spraying. Addit Manuf 2022;59:103159. https://doi.org/10.1016/j.addma.2022.103159.
[18] Kromoser B, Huber P. Pneumatic formwork systems in structural engineering. Adv Mater Sci Eng 2016;2016:1–13. https://doi.org/10.1155/2016/4724036.
[19] Popescu M, Rippmann M, Liew A, Reiter L, Flatt RJ, Van Mele T, et al. Structural design, digital fabrication and construction of the cable-net and knitted formwork of the KnitCandela concrete shell. Structures 2021;31:1287–99. https://doi.org/10.1016/j.istruc.2020.02.013.
[20] Yang W, Li Z-M, Shi W, Xie B-H, Yang M-B. Review on auxetic materials. J Mater Sci 2004;39:3269–79. https://doi.org/10.1023/B:JMSC.0000026928.93231.e0.
[21] Gan Z, Zhuge Y, Thambiratnam DP, Chan THT, Zahra T, Asad M. Recent advances in auxetics: applications in cementitious composites. Int J Prot Struct 2022;13:295–316. https://doi.org/10.1177/20414196211062620.
[22] Ren X, Das R, Tran P, Ngo TD, Xie YM. Auxetic metamaterials and structures: a review. Smart Mater Struct 2018;27:023001. https://doi.org/10.1088/1361-665X/aaa61c.
[23] Shukla S, Behera BK. Auxetic fibrous structures and their composites: a review. Compos Struct 2022;290:115530. https://doi.org/10.1016/j.compstruct.2022.115530.
[24] Bohara RP, Linforth S, Ghazlan A, Nguyen T, Remennikov A, Ngo T. Performance of an auxetic honeycomb-core sandwich panel under close-in and far-field detonations of high explosive. Compos Struct 2022;280:114907. https://doi.org/10.1016/j.compstruct.2021.114907.
[25] Zhong R, Ren X, Yu Zhang X, Luo C, Zhang Y, Min Xie Y. Mechanical properties of concrete composites with auxetic single and layered honeycomb structures. Constr Build Mater 2022;322:126453. https://doi.org/10.1016/j.conbuildmat.2022.126453.
[26] Momoh EO, Jayasinghe A, Hajsadeghi M, Vinai R, Evans KE, Kripakaran P, et al. A state-of-the-art review on the application of auxetic materials in cementitious composites. ThinWalled Struct 2024;196:111447. https://doi.org/10.1016/j.tws.2023.111447.
[27] Prawoto Y. Seeing auxetic materials from the mechanics point of view: a structural review on the negative Poisson's ratio. Comput Mater Sci 2012;58:140–53. https://doi.org/10.1016/j.commatsci.2012.02.012.

[28] Yan H, Zhang Y, Teng XC, Jiang WZ, Xie YM, Wu WW, et al. 3D compression-twist lattice metamaterials for surface reconfigurability of future architecture. Compos Struct 2024;337:118075. https://doi.org/10.1016/j.compstruct.2024.118075.
[29] Robert McNeel & Associates. Rhino 7 for Windows. 2021.
[30] Preisinger C. Karamba 3D: parametric engineering- user manual. 2019.
[31] Makki M., Showkatbakhsh M., Song Y. Wallacei: Primer 2.0. 2019.
[32] Makki M, Showkatbakhsh M, Tabony A, Weinstock M. Evolutionary algorithms for generating urban morphology: variations and multiple objectives. Int J Archit Comput 2019;17:5–35. https://doi.org/10.1177/1478077118777236.